Engineering

Electrical Engineering fields

Okayama University *Year* 1997

An approach to real-time position estimation at zero and low speed for a PM motor based on saliency

Satoshi Ogasawara
Okayama University

Hirofumi Akagi
Okayama University

An Approach to Real-Time Position Estimation at Zero and Low Speed for a PM Motor Based on Saliency

Satoshi Ogasawara, *Senior Member, IEEE*, and Hirofumi Akagi, *Fellow, IEEE*

***Abstract*—This paper presents a magnetic saliency-based position estimation approach for a permanent magnet (PM) motor fed by a voltage-source pulsewidth modulation (PWM) inverter. The proposed real-time estimation algorithm detects motor current harmonics and calculates the inductance matrix, including rotor position information. Position estimation can be performed every period of PWM or carrier cycle. An experimental system using an interior permanent magnet (IPM) synchronous motor has been constructed. Experimental results verify that position estimation within 10° in electrical angle is obtained at standstill and at speeds as low as 1 r/min by the proposed approach.**

***Index Terms*—Interior permanent magnet synchronous motor, magnetic saliency, sensorless drive.**

I. Introduction

IN RECENT years, significant attention has been paid to removing rotor position sensors from ac motor drive systems with a position-closed loop [1]–[8]. The rotor position estimation methods of a permanent magnet (PM) synchronous motor can be classified into the following two groups:

1) based on the back EMF produced in the stator windings [1], [2];
2) based on magnetic saliency [3]–[6].

Conventional position estimation based on detection of back EMF is suitable for middle- and high-speed applications. However, at low speed and standstill, the EMF is too small to achieve accurate position estimation. On the other hand, magnetic saliency-based position estimation can be potentially employed at any speed, including zero speed.

Lorenz *et al.*, have proposed a sophisticated approach to estimation of flux, position, and speed at zero and low speed in ac motors [4], [5]. The approach is based on tracking the magnetic saliency via inverter-generated high-frequency signal injection with demodulation incorporating heterodyning and a closed-loop observer.

This paper presents a magnetic saliency-based position estimation approach for a PM motor fed by a voltage-source pulsewidth modulation (PWM) inverter. The proposed real-time estimation algorithm detects motor current harmonics and calculates the inductance matrix, including rotor position information. Position estimation can be performed every period of PWM, without any special signal injection.

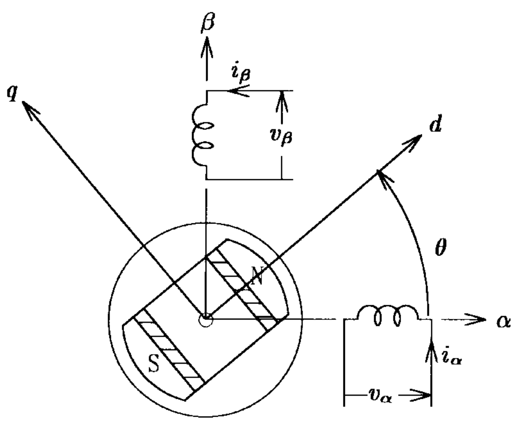

Fig. 1. Model of salient PM motor.

An experimental system consisting of an interior permanent magnet (IPM) synchronous motor and a voltage-source PWM inverter has been constructed and tested to verify the effectiveness and versatility of the approach to position estimation at zero and low speed. The IPM motor has the magnetic saliency of the q-axis inductance being larger than the d-axis inductance. Experimental results show that the proposed approach has the capability of estimating the rotor position at standstill and at speeds as low as 1 r/min.

II. Harmonic Model of PM Motor

Fig. 1 shows the simplified model of a PM motor with magnetic saliency. The equations describing the PM motor are given by

$$\begin{bmatrix} v_\alpha \\ v_\beta \end{bmatrix} = r\begin{bmatrix} i_\alpha \\ i_\beta \end{bmatrix} + \begin{bmatrix} L_0 + L_1\cos 2\theta & L_1 \sin 2\theta \\ L_1 \sin 2\theta & L_0 - L_1\cos 2\theta \end{bmatrix} \frac{d}{dt}\begin{bmatrix} i_\alpha \\ i_\beta \end{bmatrix} + \frac{d\theta}{dt}\left(2L_1\begin{bmatrix} -\sin 2\theta & \cos 2\theta \\ \cos 2\theta & \sin 2\theta \end{bmatrix}\begin{bmatrix} i_\alpha \\ i_\beta \end{bmatrix} + \phi_{\mathrm{mag}}\begin{bmatrix} -\sin\theta \\ \cos\theta \end{bmatrix}\right) \quad (1)$$

where

$$L_0 = \frac{L_d + L_q}{2}, \quad L_1 = \frac{L_d - L_q}{2}. \quad (2)$$

Paper IPCSD 97–59, presented at the 1996 Industry Applications Society Annual Meeting, San Diego, CA, October 6–10, and approved for publication in the IEEE Transactions on Industry Applications by the Industrial Drives Committee of the IEEE Industry Applications Society. Manuscript released for publication August 12, 1997.

The authors are with the Department of Electrical Engineering, Okayama University, Okayama, 700 Japan (e-mail: ogasawara@elec.okayama-u.ac.jp; akagi@elec.okayama-u.ac.jp).

Publisher Item Identifier S 0093-9994(98)00880-9.

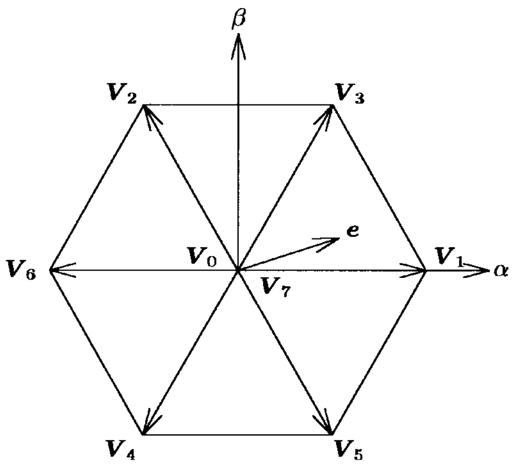

Fig. 2. Voltage vectors of inverter output.

The equations can be simplified by applying the space vector theory:

$$\boldsymbol{v} = r\boldsymbol{i} + \boldsymbol{L}\frac{d\boldsymbol{i}}{dt} + \boldsymbol{e}_0. \tag{3}$$

Here, the inductance matrix is represented by

$$\boldsymbol{L} = \begin{bmatrix} L_0 + L_1\cos 2\theta & L_1 \sin 2\theta \\ L_1 \sin 2\theta & L_0 - L_1 \cos 2\theta \end{bmatrix} \tag{4}$$

and it contains the rotor position information of the PM motor.

When the PM motor is driven by a voltage-source PWM inverter, the motor current contains a small amount of harmonic current. The voltage and current vectors can be separated into the fundamental and harmonic components as follows:

$$\boldsymbol{v} = \overline{\boldsymbol{v}} + \tilde{\boldsymbol{v}} \tag{5}$$

$$\boldsymbol{i} = \overline{\boldsymbol{i}} + \tilde{\boldsymbol{i}}. \tag{6}$$

Because the resistive voltage drop can be disregarded, the harmonic equivalent circuit can be approximated by the inductance:

$$\tilde{\boldsymbol{v}} = \boldsymbol{L}\frac{d\tilde{\boldsymbol{i}}}{dt}. \tag{7}$$

The above equation indicates that the inductance matrix can be calculated from the harmonic components of the motor voltage and current vectors, so that the rotor position can be estimated.

III. Harmonic Voltage and Current Vectors

A three-phase voltage-source inverter can output eight discrete voltage vectors, including two zero vectors, as shown in Fig. 2. The PWM inverter has the capability of producing an output voltage vector by selecting the discrete voltage vectors selectively in a modulation period. The average voltage vector is

$$\boldsymbol{e} = \sum \zeta_k \boldsymbol{V}_k \tag{8}$$

where ζ_k means the time ratio of $\boldsymbol{V}_k$ to the modulation period:

$$\zeta_k = \frac{t_k}{T}. \tag{9}$$

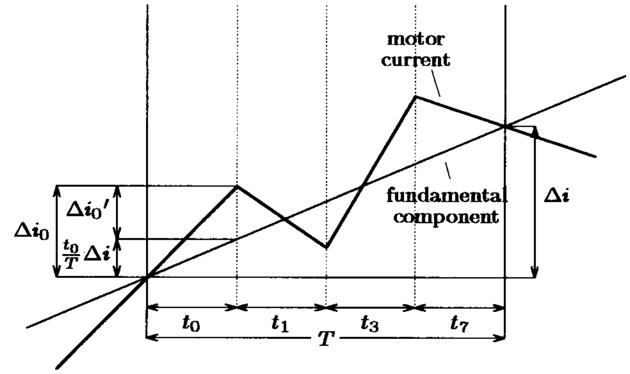

Fig. 3. Variation of motor current.

Therefore, the harmonic voltage vector is equal to a difference between the inverter output voltage vector and the average output voltage vector:

$$\boldsymbol{V}_k' = \boldsymbol{V}_k - \boldsymbol{e}. \tag{10}$$

On the other hand, applying the approximation of (7) implies the motor current changes linearly, as shown in Fig. 3. Since the motor current includes both the harmonic and fundamental components, the two components should be separated from each other. The current variation for modulation period is shown by

$$\boldsymbol{\Delta i} = \sum \boldsymbol{\Delta i}_k \tag{11}$$

where $\boldsymbol{\Delta i}_0, \cdots, \boldsymbol{\Delta i}_7$ are the current variations for the intervals of $t_0, \cdots, t_7$, respectively. Assuming that the fundamental component changes linearly in a modulation period, the harmonic component of the current variation can be separated by the following equation:

$$\boldsymbol{\Delta i}_k' = \boldsymbol{\Delta i}_k - \zeta_k \boldsymbol{\Delta i}. \tag{12}$$

As a result, we can extract only harmonic components of the voltage and current vectors.

IV. Estimation of Inductance Matrix and Rotor Position

From (7), a relationship between the harmonic components of the voltage vector and the current variation vector is given by

$$\boldsymbol{L}\boldsymbol{\Delta i}_k' = \boldsymbol{V}_k' t_k. \tag{13}$$

Lumping the above equations together over a modulation period gives the following equation:

$$\boldsymbol{L}[\boldsymbol{\Delta i}_0' \quad \boldsymbol{\Delta i}_1' \quad \cdots \quad \boldsymbol{\Delta i}_7'] = [\boldsymbol{V}_0' t_0 \quad \boldsymbol{V}_1' t_1 \quad \cdots \quad \boldsymbol{V}_7' t_7]. \tag{14}$$

The transposed equation is

$$\begin{bmatrix} \boldsymbol{\Delta i}_0'^T \\ \boldsymbol{\Delta i}_1'^T \\ \vdots \\ \boldsymbol{\Delta i}_7'^T \end{bmatrix} \boldsymbol{L}^T = \begin{bmatrix} \boldsymbol{V}_0'^T t_0 \\ \boldsymbol{V}_1'^T t_1 \\ \vdots \\ \boldsymbol{V}_7'^T t_7 \end{bmatrix}. \tag{15}$$

Therefore, the inductance matrix can be calculated as follows:

$$
\begin{aligned}
\boldsymbol{L}^T &= \begin{bmatrix} \boldsymbol{\Delta i}_0'^T \\ \boldsymbol{\Delta i}_1'^T \\ \vdots \\ \boldsymbol{\Delta i}_7'^T \end{bmatrix}^{\mathrm{LM}} \begin{bmatrix} \boldsymbol{V}_0'^T t_0 \\ \boldsymbol{V}_1'^T t_1 \\ \vdots \\ \boldsymbol{V}_7'^T t_7 \end{bmatrix} \\
&= \begin{bmatrix} L_{11} & L_{12} \\ L_{21} & L_{22} \end{bmatrix}^T \\
&= \begin{bmatrix} L_0 + L_1 \cos 2\theta & L_1 \sin 2\theta \\ L_1 \sin 2\theta & L_0 - L_1 \cos 2\theta \end{bmatrix}.
\end{aligned} \tag{16}
$$

Here, the "LM" in the above equation is the *left pseudoinverse* operator [9], and it performs the following calculation:

$$
\boldsymbol{H}^{\mathrm{LM}} = (\boldsymbol{H}^T \boldsymbol{H})^{-1} \boldsymbol{H}^T. \tag{17}
$$

Therefore, the rotor position can be calculated from the inductance matrix:

$$
2\theta = \tan^{-1} \frac{L_{12} + L_{21}}{L_{11} - L_{22}}. \tag{18}
$$

The inverse matrix of $\boldsymbol{H}^T \boldsymbol{H}$ must be existent, otherwise we cannot calculate the left pseudoinverse matrix in (16). The matrix of $\boldsymbol{H}^T \boldsymbol{H}$ is calculated as follows:

$$
\begin{aligned}
&\boldsymbol{H}^T \boldsymbol{H} \\
&= \begin{bmatrix} \Delta i_{0\alpha}' & \Delta i_{1\alpha}' & \cdots & \Delta i_{7\alpha}' \\ \Delta i_{0\beta}' & \Delta i_{1\beta}' & \cdots & \Delta i_{7\beta}' \end{bmatrix} \begin{bmatrix} \Delta i_{0\alpha}' & \Delta i_{0\beta}' \\ \Delta i_{1\alpha}' & \Delta i_{1\beta}' \\ \vdots & \vdots \\ \Delta i_{7\alpha}' & \Delta i_{7\beta}' \end{bmatrix} \\
&= \begin{bmatrix} \sum \Delta i_{k\alpha}'^2 & \sum \Delta i_{k\alpha}' \cdot \Delta i_{k\beta}' \\ \sum \Delta i_{k\alpha}' \cdot \Delta i_{k\beta}' & \sum \Delta i_{k\beta}'^2 \end{bmatrix}.
\end{aligned} \tag{19}
$$

If all α or β components in $\boldsymbol{\Delta i}_k'$ are zero, the determinant of $\boldsymbol{H}^T \boldsymbol{H}$ becomes zero. Similarly, if all of them are linearly dependent, the inverse matrix is not existent because $\det(\boldsymbol{H}^T \boldsymbol{H}) = 0$.Therefore, PWM control should be modified so that all of them are not linearly dependent vectors.

Fig. 4(a) shows a timing chart in a conventional sinusoidal PWM scheme. Comparison of the voltage references v_u^*, v_v^*, and v_w^* with a triangular carrier determines the output voltage vector. In this case, $\boldsymbol{V}_0, \boldsymbol{V}_1, \boldsymbol{V}_3$, and $\boldsymbol{V}_7$ are output vectors for t_0, t_1, t_3, and t_7, respectively. The following equation expresses the average voltage vector during a modulation period:

$$
\boldsymbol{e} = \zeta_0 \boldsymbol{V}_0 + \zeta_1 \boldsymbol{V}_1 + \zeta_3 \boldsymbol{V}_3 + \zeta_7 \boldsymbol{V}_7 \tag{20}
$$

where

$$
\zeta_0 + \zeta_1 + \zeta_3 + \zeta_7 = 1. \tag{21}
$$

For example, when the average voltage vector exists on the centroid of a triangle formed by $\boldsymbol{V}_0, \boldsymbol{V}_1, \boldsymbol{V}_3$, and $\boldsymbol{V}_7$ in Fig. 4(b), the time ratios are

$$
\zeta_0 + \zeta_7 = \zeta_1 = \zeta_3 = \tfrac{1}{3}. \tag{22}
$$

In this case, $\boldsymbol{\Delta i}_0', \boldsymbol{\Delta i}_1', \boldsymbol{\Delta i}_3'$, and $\boldsymbol{\Delta i}_7'$ are linearly independent of each other, except that $\boldsymbol{\Delta i}_0'$ is linearly dependent on $\boldsymbol{\Delta i}_7'$.As a result, we can calculate the inductance matrix and estimate the rotor position.

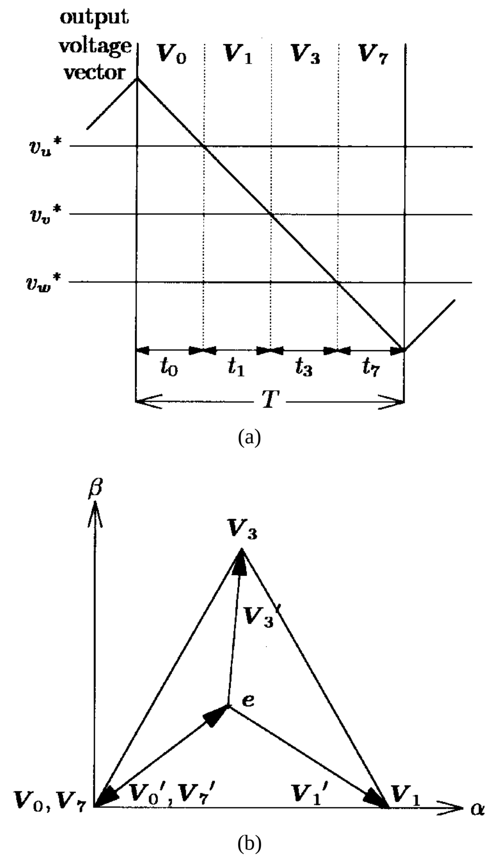

Fig. 4. Conventional sinusoidal PWM scheme. (a) Comparing voltage references with triangle. (b) Voltage vectors.

However, it is not necessary to output $\boldsymbol{V}_3$ when the average voltage vector exists on the α axis, i.e., $v_v^* = v_w^*$.In this case, $\boldsymbol{\Delta i}_1', \boldsymbol{\Delta i}_0'$, and $\boldsymbol{\Delta i}_7'$ are linearly dependent on each other, because $\boldsymbol{V}_1'$ moves in the opposite direction of $\boldsymbol{V}_0'$ or $\boldsymbol{V}_7'$. Due to $\det(\boldsymbol{H}^T \boldsymbol{H}) = 0$, it is impossible to calculate the inductance matrix $\boldsymbol{L}$.

In addition, $\zeta_0 + \zeta_7$ is close to unity, and ζ_1 and ζ_3 are very small, when the average voltage vector $\boldsymbol{e}$ exists near the origin in the α–β coordinates. In this area, the position estimation cannot be performed with enough accuracy, because all components in $\boldsymbol{\Delta i}_k'$ are zero or a small value. The fact mentioned above shows that the conventional sinusoidal PWM scheme is not applicable to the proposed position estimation.

V. Modification of PWM Control

In order to perform precise position estimation, the authors propose a novel PWM scheme using redundant voltage vectors. The average voltage vector during a modulation period can be expressed by

$$
\boldsymbol{e} = \sum s_k \zeta_k \boldsymbol{V}_k \tag{23}
$$

$$
\sum s_k \zeta_k = 1. \tag{24}
$$

Here, s_k, which takes a value of 1 or 0 during the modulation period, indicates whether $\boldsymbol{V}_k$ is selected as an output vector

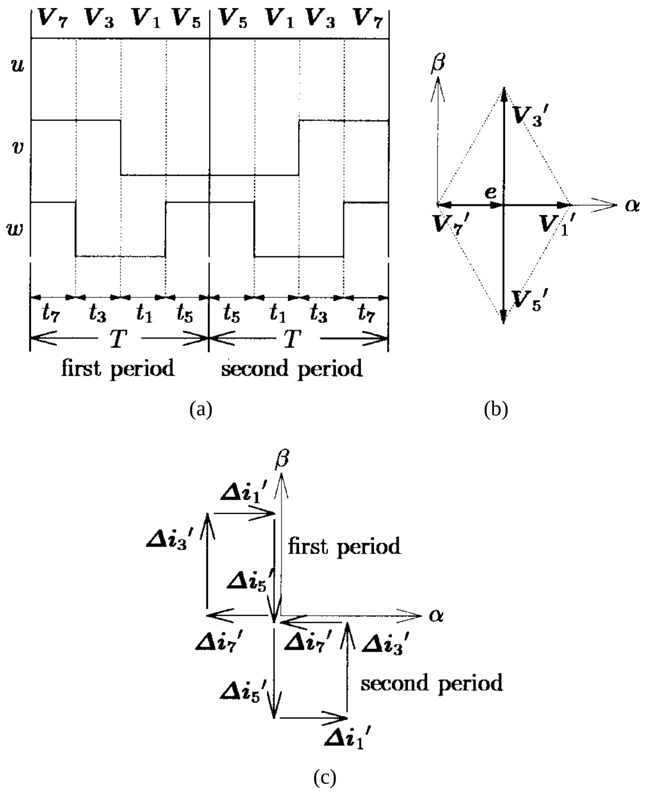

Fig. 5. PWM scheme using redundant voltage vectors. The average voltage vector exists on the α axis. (a) PWM pattern. (b) Harmonic voltage vectors. (c) Trajectory of harmonic current vector.

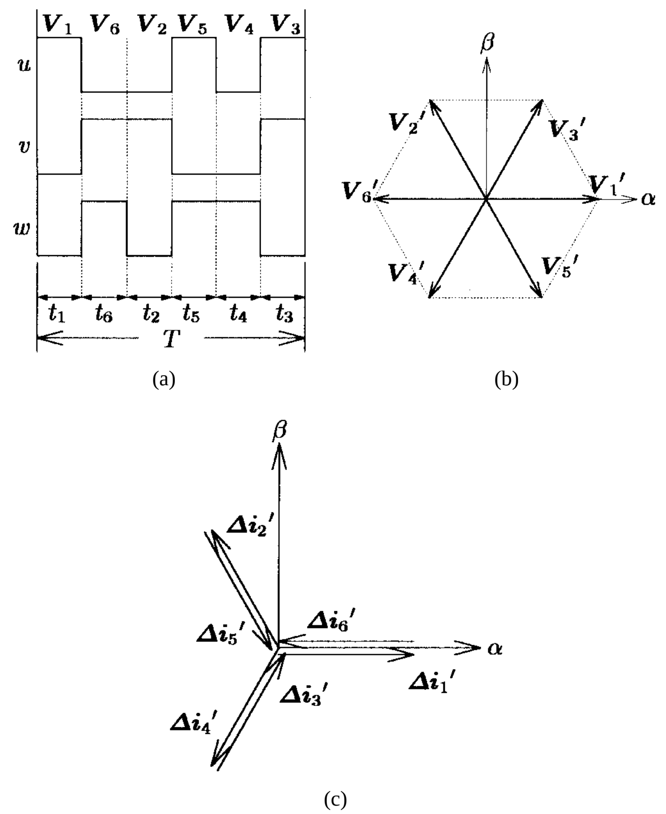

Fig. 6. PWM scheme using redundant voltage vectors. The average voltage vector exists on the origin of the α–β coordinate. (a) PWM pattern. (b) Harmonic voltage vectors. (c) Trajectory of harmonic current vectors.

or not, respectively. Lumping the equations together gives the following equation:

$$\begin{bmatrix} e_\alpha \\ e_\beta \\ 1 \end{bmatrix} = \begin{bmatrix} s_0 V_{0\alpha} & s_1 V_{1\alpha} & \cdots & s_7 V_{7\alpha} \\ s_0 V_{0\beta} & s_1 V_{1\beta} & \cdots & s_7 V_{7\beta} \\ s_0 & s_1 & \cdots & s_7 \end{bmatrix} \begin{bmatrix} \zeta_0 \\ \zeta_1 \\ \vdots \\ \zeta_7 \end{bmatrix}. \tag{25}$$

In the above equation, ζ_k has to be decided so that the PWM inverter outputs the average voltage vector $\boldsymbol{e}$ during the modulation period. No general solution to (25) exists because the number of unknown variables is more than the number of equations. However, introduction of a *right pseudoinverse* matrix [9] allows a solution to ζ_k as follows:

$$\begin{bmatrix} \zeta_0 \\ \zeta_1 \\ \vdots \\ \zeta_7 \end{bmatrix} = \begin{bmatrix} s_0 V_{0\alpha} & s_1 V_{1\alpha} & \cdots & s_7 V_{7\alpha} \\ s_0 V_{0\beta} & s_1 V_{1\beta} & \cdots & s_7 V_{7\beta} \\ s_0 & s_1 & \cdots & s_7 \end{bmatrix}^{\mathrm{RM}} \begin{bmatrix} e_\alpha \\ e_\beta \\ 1 \end{bmatrix} \tag{26}$$

where

$$\boldsymbol{F}^{\mathrm{RM}} = \boldsymbol{F}^T(\boldsymbol{F}\boldsymbol{F}^T)^{-1}. \tag{27}$$

As a result of the calculation, one can decide a suitable PWM pattern under any combination of $\boldsymbol{V}_k$ during the modulation period.

Fig. 5(a) shows a PWM pattern produced when the average voltage vector $\boldsymbol{e}$ exists on the α axis. Note that $\boldsymbol{V}_5$ is selected during an interval of time, different from $\boldsymbol{V}_0$ being selected during the corresponding interval in the conventional sinusoidal PWM scheme. As shown in Fig. 5(b), $\boldsymbol{V}_3'$ and $\boldsymbol{V}_5'$ produce β-axis components in the harmonic current vectors, while $\boldsymbol{V}_1'$ and $\boldsymbol{V}_7'$ produce α-axis components. Fig. 5(c) shows the trajectory of the harmonic current vector. The trajectory starts from the origin toward the left at the beginning of the first modulation period. Since the harmonic current vector changes toward the direction near that of the corresponding harmonic voltage vector, the trajectory draws a rectangle and returns to the origin at the end of the first period. None of the vectors $\boldsymbol{\Delta i}_7', \boldsymbol{\Delta i}_3', \boldsymbol{\Delta i}_1'$, and $\boldsymbol{\Delta i}_5'$ are linearly dependent in the first period. The rotor position, therefore, can be estimated by the proposed algorithm, based on the harmonic component of the current variation, independent of the location of the average voltage vector. Note that the sum of the harmonic current vectors in the first modulation period shown in Fig. 5 is not equal to a zero vector. In order to compensate for the deviation, the sequence of selecting the voltage vectors should be modified as shown in the second modulation period.

Fig. 6 shows a PWM scheme where the average voltage vector exists on the origin of the α-β coordinate. This situation corresponds to the case of position estimation at standstill. Each voltage vector is output for 1/6 of the modulation period. Note that the inverter selects neither $\boldsymbol{V}_0$ nor $\boldsymbol{V}_7$.The sequence is scheduled so that the trajectory of the harmonic current vectors starts from the origin at the beginning of the modulation period and returns to the origin at the end. Since none of the harmonic current vectors are linearly dependent, the position estimation can be performed even at a standstill.

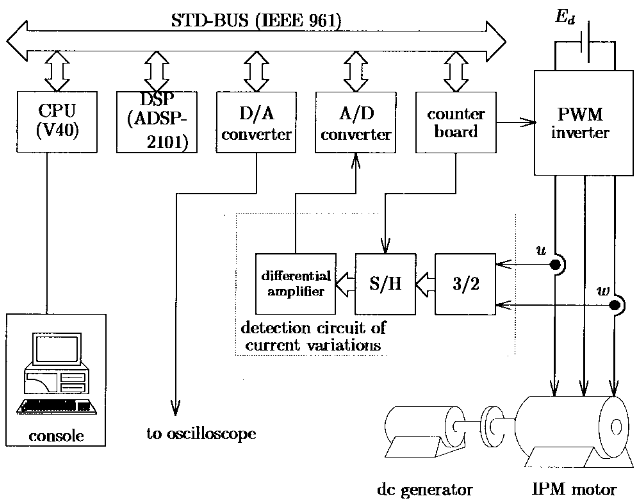

Fig. 7. Configuration of experimental system.

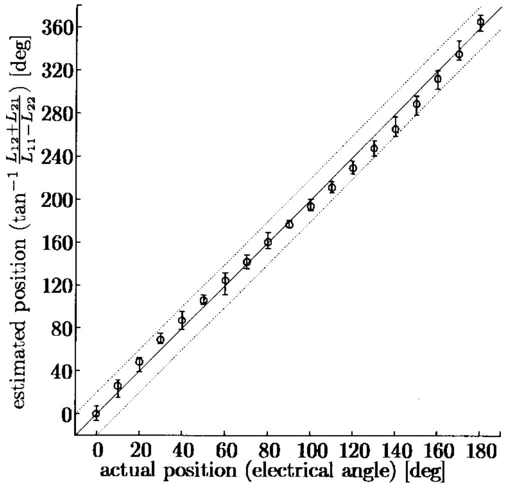

Fig. 8. Experimental result at standstill.

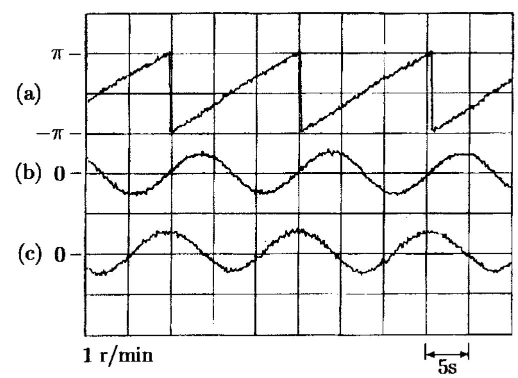

Fig. 9. Experimental result at 1 r/min. (a) Estimated position $\tan^{-1}(L_{12}+L_{21}/L_{11}-L_{22})$. (b) $L_{12}+L_{21}$. (c) $L_{11}-L_{22}$.

TABLE I
IPM MOTOR PARAMETERS

number of poles		4	
resistance	r	15	Ω
d-axis inductance	L_d	125	mH
q-axis inductance	L_q	206	mH
rated power		100	W
rated speed		1500	rpm
modulation period	T	333	μs
dc voltage	E_d	280	V

VI. EXPERIMENTAL RESULT

Fig. 7 shows the configuration of the experimental system, consisting of a V40 CPU and a digital signal processor (DSP) (ADSP-2101). The V40 CPU supervises the whole operation of the system, and the DSP calculates the PWM pattern, the inductance matrix, and the estimated rotor position.

The counter board is capable of synthesizing the PWM signal of the inverter, following the PWM pattern calculated by the DSP. The PWM signal in a modulation period consists of six voltage vectors in any order. The detected motor currents are transformed from three-phase to α–β components. The counter board also generates the sample/hold signals by which the transformed motor currents are held just before every switching, so that the switching noises do not affect the signals being held. Each current variation in (11) is applied to an A/D converter through a differential amplifier. The detection circuit consisting of the sample/hold amplifiers and the differential amplifiers makes a significant contribution to precisely detecting each current variation.

Table I shows the parameters of the PM motor used in the experimental system. Since the tested motor is an IPM motor, it has the saliency of the q-axis inductance being larger than d-axis inductance. The DSP can perform all the calculations for the inductance matrix and rotor position, as well as PWM control within a modulation period of 333 μs. In the following experimental results, the PWM pattern shown in Fig. 6 is used to achieve the rotor position estimation at standstill and in the low-speed range.

Fig. 8 shows the experimental result of the position estimation proposed in this paper at standstill. A circle "○" and the corresponding vertical bar mean the average value and existing range of estimated position, respectively, obtained from 20 trials at a rotor position. The experimental result shows that the real-time position estimation is achieved at standstill with such satisfactory accuracy as to add a position-closed loop to a PM motor drive system. Note that the vertical axis is not θ, but 2θ. It would be possible to distinguish the polarity of the rotor magnetic pole by means of another technique based on magnetic saturation [3].

Fig. 9 shows another experimental result at 1 r/min. The conventional position estimation based on back EMF would not be applicable at such a low speed. In this experiment, the inverter is controlled to continue to select the zero average voltage vector, and the rotor of the IPM motor is rotated by the dc generator, which is directly connected to the shaft. These experimental results show the effectiveness and versatility of the position estimation proposed in this paper.

VII. CONCLUSION

This paper has proposed an approach to real-time position estimation based on magnetic saliency. A novel PWM scheme using redundant voltage vectors has been proposed to achieve the position estimation. Experimental results have demonstrated that the proposed approach has the capacity of estimating the rotor position with an error of less than 10° in electrical angle at standstill and at extremely slow speeds, as low as 1 r/min. The proposed approach is applicable to other ac motors with magnetic saliency, such as synchronous reluctance motors. In addition, it identifies inductance parameters in real time for motor control, without requiring user input of machine constants. The authors plan to construct a position-sensorless IPM motor system with a position-closed loop based on the proposed approach in the next stage.

References

[1] K. Iizuka, H. Uzuhashi, M. Kano, T. Endo, and K. Mori, "Microcomputer control for sensorless brushless motor," *IEEE Trans. Ind. Applicat.*, vol. IA-21, pp. 595–601, May/June 1985.

[2] S. Ogasawara and H. Akagi, "An approach to position sensorless drive for brushless dc motors," *IEEE Trans. Ind. Applicat.*, vol. 27, pp. 928–933, Sept./Oct. 1991.

[3] N. Matsui and T. Takeshita, "A novel starting method of sensorless salient-pole brushless motor," in *Proc. IEEE-IAS Annu. Meeting*, 1994, pp. 386–392.

[4] P. L. Jansen and R. D. Lorenz, "Transducerless position and velocity estimation in induction and salient AC machines," in *Proc. IEEE-IAS Annu. Meeting*, 1994, pp. 488–495.

[5] P. L. Jansen, M. J. Corley, and R. D. Lorenz, " Flux, position, and velocity estimation in AC machines at zero and low speed via tracking of high frequency saliency," in *Proc. EPE'95*, Seville, Spain, 1995, vol. 3, pp. 154–159.

[6] S. Kondo, A. Takahashi, and T. Nishida, "Armature current locus based estimation method of rotor position of permanent magnet synchronous motor without mechanical sensor," in *Proc. IEEE-IAS Annu. Meeting*, 1995, pp. 55–60.

[7] T. Matsuo and T. A. Lipo, "Rotor position detection scheme for synchronous reluctance motor based on current measurements," *IEEE Trans. Ind. Applicat.*, vol. 31, pp. 860–868, July/Aug. 1995.

[8] K. D. Hurst and T. G. Habetler, "Sensorless speed measurement using current harmonic spectral estimation in induction machine drives," *IEEE Trans. Power Electron.*, vol. 11, pp. 66–73, Jan. 1996.

[9] S. Wolfram, *Mathematica—A System for Doing Mathematics by Computer*, 2nd ed. Reading, MA: Addison-Wesley, 1991.

Satoshi Ogasawara (A'87–M'93–SM'97) was born in Kagawa Prefecture, Japan, in 1958. He received the B.S., M.S., and Dr.Eng. degrees in electrical engineering from Nagaoka University of Technology, Niigata, Japan, in 1981, 1983, and 1990, respectively.

From 1983 to 1992, he was a Research Associate at Nagaoka University of Technology. Since 1992, he has been with the Department of Electrical Engineering, Okayama University, Okayama, Japan, where he is currently an Associate Professor. His present reseach interests are ac motor drives systems and static power converters.

Dr. Ogasawara received the 1996 Prize Paper Awards of the Industrial Power Converter Committee and Industrial Drive of the IEEE Industry Applications Society in 1996 and 1997. He is a member of the Institute of Electrical Engineers of Japan.

Hirofumi Akagi (M'87–SM'94–F'96) was born in Okayama-city, Japan, in 1951. He received the B.S. degree from Nagoya Institute of Technology, Nagoya, Japan, in 1974 and the M.S. and Ph.D. degrees from Tokyo Institute of Technology, Tokyo, Japan, in 1976 and 1979, respectively, all in electrical engineering.

In 1979, he joined Nagaoka University of Technology, Niigata, Japan, as an Assistant Professor in the Department of Electrical Engineering, where he later became an Associate Professor. In 1987, he was a Visiting Scientist at the Massachusetts Institute of Technology, Cambridge, for ten months. Since 1991, he has been a Full Professor in the Department of Electrical Engineering, Okayama University, Okayama, Japan. From March to August 1996, he was a Visiting Professor at the University of Wisconsin, Madison, and the Massachusetts Institute of Technology. His research interests include ac motor drives, high-frequency resonant inverters for induction heating and corona discharge treatment, and utility applications of power electronics, such as active filters, static var compensators, and FACTS devices.

Dr. Akagi is the recipient of seven IEEE Industry Applications Society and Committee Prize Paper Awards, including the IEEE Industry Applications Society 1991 First Prize Paper Award. He is a Distinguished Lecturer of the IEEE/IAS for 1998–1999.